



Dissolved organic matter in digested piggery wastewater from combined treatment process

Shouliang Huo^a, Beidou Xi^{a,*}, Fengyu Zan^{a,b}, Feng Zeng^a, Jingtian Zhang^a, Jing Su^a

^aState Key Laboratory of Environmental Criteria and Risk Assessment, Chinese Research Academy of Environmental Science, Beijing 100012, China

Tel./Fax: +86 10 84913133; email: xibeidou@263.net

^bCollege of Environmental Science and Engineering, Anhui Normal University, Wuhu, Anhui 241000, China

Received 29 February 2012; Accepted 7 August 2012

ABSTRACT

The temporal and spatial variation of dissolved organic matter in the processes of hydrolytic acidification and biological contact oxidation during post-treatment of digested piggery wastewater were characterized systematically by means of ion chromatography, fluorescence spectra, and ultraviolet spectra in this study. The highest removal efficiencies of chemical oxygen demand and nitrogen have been achieved when the 1/3 effluent of biological contact oxidation reactor was backflow into the reactor of hydrolytic acidification. It was found that the concentrations of total organic acids were 283.6 mg/L at the first 2 h of hydrolytic reaction and 305.5 mg/L at the beginning of recirculation between the two reactors and then decreased to around 200 mg/L and keep stable. The results of synchronous and three-dimensional excitation–emission matrix fluorescence spectroscopy revealed that the protein-like fluorescence peaks were identified in the hydrolytic acidification reactor and their intensities increased gradually along with hydrolytic time increasing. Moreover, the fulvic acid-like fluorescence peaks in biological contact oxidation reactor were observed, and the intensity increased gradually. The synchronous intensity of 277 nm wavelength was significantly correlated with the total organic acids concentration. Variation of $SUVA_{254}$ and E_{253}/E_{203} during the hydrolytic acidification process indicated that concentrations of aromatic and unsaturated compounds slightly increase and those aromatic compounds are not stable. However, $SUVA_{254}$ and E_{253}/E_{203} decreased rapidly in the biological contact oxidation reactor, which suggested that easily degradable organic matters had been consumed rapidly.

Keywords: Anaerobic digested wastewater; Dissolved organic matter; Ion chromatography; Three-dimensional fluorescence spectroscopy; Ultraviolet spectra

1. Introduction

Development of intensive and large-scale pig breeding industry has brought enormous economic benefits in China. However, the pollution of concentrated piggery wastewater has attracted wide attention. It is estimated that piggery wastewater is

seriously polluted with BOD ranging from 2,000 to 8,000 mg/L and chemical oxygen demand (COD) between 5,000 and 20,000 mg/L. During the past years, many aerobic and combined anaerobic–aerobic processes were used in piggery wastewater treatment, such as activated sludge, rotating biological contactors, biofilter, oxidation ditches, and anoxic/aerobic process [1,2]. In recent years, the piggery wastewater treatment in sequencing batch reactor

*Corresponding author.

(SBR) and intermittent aeration were widely used [3–13]. Although, most of them can achieve good removal efficiencies including 95% of COD and total nitrogen (TN) removal rates, and 90% of total phosphorus removal rate [5–8,10], a long hydraulic retention time of 9–16 days was needed [5,14,15]. Anaerobic digestion of piggery wastewater was proved to be an effective method to remove organic pollutants. However, digested piggery wastewater containing high concentrations of organic pollutants and $\text{NH}_3\text{-N}$, low alkalinity, poor biodegradability, low C/N, which restrict the removal efficiency and stability in the post-treatment process [16]. And the removal efficiencies of COD and $\text{NH}_3\text{-N}$ using biological processes (e.g. SBR or biological contact oxidation) alone are inefficient, due to lack of carbon sources in the denitrification phase [16]. Hydrolytic acidification has been considered as an efficient pretreatment process in treating high concentrations of organic pollutants and $\text{NH}_3\text{-N}$ by increasing the biodegradability of effluent. Therefore, the combined process of hydrolytic acidification and biological contact oxidation was introduced to deal with digested piggery wastewater to achieve better treatment performance for $\text{NH}_3\text{-N}$ and COD.

Dissolved organic matter (DOM) including aromatic and aliphatic organic compound plays a significant role in the wastewater treatment process, especially the fractions of small molecular acids. Although some emphasis has been focused on variation of DOM concentrations using BOD_5 , COD, and dissolved organic carbon (DOC), the information about DOM composition and structure in the digested wastewater treatment process have rarely been reported. Moreover, some advanced analysis techniques such as carbon nuclear magnetic resonance (^{13}C NMR) spectroscopy were used to quantify specific DOM compounds often requires complex sample preparation [17]. Analysis of chromophoric (light absorbing) and fluorophoric (light emitting) moieties in water sample is becoming increasingly widespread, due to the advantage of short testing time, high sensitivity, simple pretreatment, and good integrity of samples. In the last 50 years, fluorescence spectra and ultraviolet spectra were applied into investigating the composition and distribution of organic matters in natural water and sewage [18–22].

The major objective of this study was to estimate the variation of DOM characteristics in the combined process of hydrolytic acidification and biological contact oxidation treating digested piggery wastewater by means of ion chromatography, fluorescence spectra and ultraviolet spectra. Moreover, the effect of operational conditions on characteristics of organic acids

and DOM was also discussed in order to provide a basis of optimizing digested wastewater treatment process and rapidly characterizing DOM.

2. Materials and methods

2.1. Experimental setup

Fig. 1 shows the schematic diagram of the two laboratory-scale reactors (hydrolytic acidification reactor and biological contact oxidation reactor) used in this study. The reactors were made of acrylic resin and had an internal diameter of 0.24 m and height of 0.8 m, providing an effective volume of 30 L. A paddle-blade stirrer was placed in the hydrolytic acidification reactor to mix the sewage completely. Influent was fed into the hydrolytic acidification reactor by a peristaltic pump from the storage tank, where the influent was mixed with a stirrer. Sewage settled 1 h after hydrolytic acidification, and the supernatant was pumped into the biological contact oxidation reactor. The media for the filter were made of combined soft and semi-soft plastic fillers, which can provide good water and gas distribution performance, and well growing biofilm.

2.2. Operating conditions

Digested piggery wastewater used in this study was collected from secondary fermentation tank in a pig farm sewage treatment plant, which located in Shunyi district of Beijing, China. The COD and $\text{NH}_3\text{-N}$ concentrations of digested piggery wastewaters were between 1,390.4 and 2,578.8 mg/L and 461.12 and 395.32 mg/L, respectively, and BOD_5/TN was very low as that reported before [1,23]. Both hydrolytic acidification reactor and biological contact oxidation reactor were operated at a cycle for 12 h including 10 h reaction time and 2 h sedimentation time. The recirculation ratio of sewage was set at 1/2, 1/3, and 1/4 of the effluent quantity after every cycle, and a water sample was collected every 1 h. The nitrogen removal performances under different recirculation ratio (1/2, 1/3, and 1/4) were also evaluated. The operations of the two reactors were automatically controlled by Programmable Logic Controller and electromagnetic valves.

2.3. Sample analysis

The wastewater samples were centrifuged with a rotating speed of $3,500 \text{ r min}^{-1}$ for 10 min under 4°C , and filtrated through glass-fiber membrane ($0.45 \mu\text{m}$)

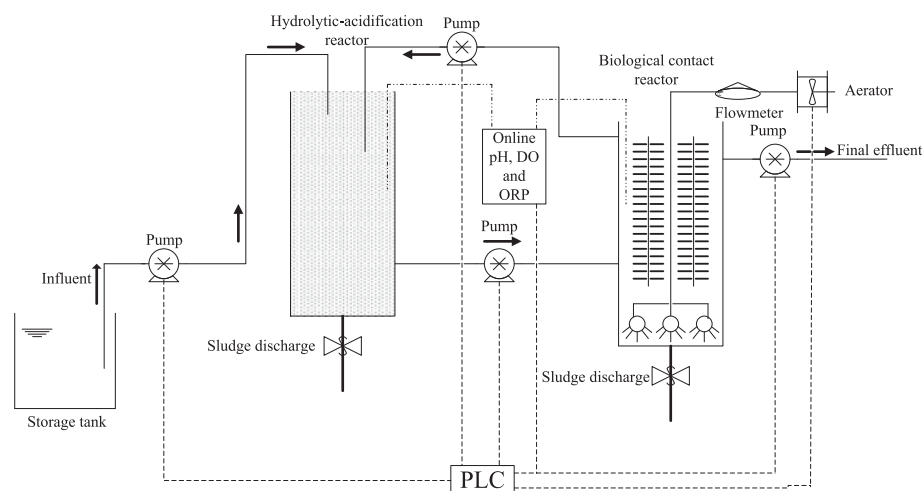


Fig. 1. Schematic diagram of combined treatment process.

to remove the suspended matters that may react with DOM. In this study, the soluble formic acid, acetic acid and propanoic acid were measured by ion chromatography, which was carried out at 0.50 mmol/L KOH of mobile phase, 1 ml/min flow rate, 35 min elution time, 2 mA suppressing current, 25 μ L injection volume [14]. Fluorescence spectra were measured by a Hitachi F-7000 fluorescence spectrometer (Hitachi High-Technologies Corporation, Japan) with a xenon lamp as the excitation source. And the fluorescence spectra of the samples were recorded using 1 cm quartz cuvettes. The excitation (E_x) and emission (E_m) slits were set to a 5 nm band-pass with a response time of 0.5 s, and scan speed was 2,400 nm min⁻¹. Each excitation–emission matrix (EEM) spectrum was generated by scanning excitation wavelengths from 200 to 400 nm, and detecting the emitted fluorescence between 280 and 500 nm [24]. The synchronous fluorescence spectra were determined at $\Delta\lambda = 30$ nm with spectral range from 260 to 550 nm [24]. Ultraviolet spectra were collected by UV-4802 (Unico-sh Corporation, China) between 200 and 700 nm with scanning distance of 0.5 nm. Specific ultraviolet absorbance ($SUVA_{254}$) was selected to characterize aromatic compounds and some refractory organics with unsaturated carbon–carbon bond [25]. Moreover, E_{253}/E_{203} was used to characterize the state of substituents on aromatic ring, with low ratio of E_{253}/E_{203} suggesting to aliphatic substituents and high ratio of E_{253}/E_{203} responses to substituents of carbonyl, carboxyl, hydroxyl and ester [26]. Therefore, the absorbance values in 203, 253, and 254 nm were measured to calculate E_{253}/E_{203} and $SUVA_{254}$ ($SUVA_{254} = E_{254} \times 100/c_{DOC}$). The software Origin 7.0 (Origin Lab Inc., USA) was employed to process the EEM data, synchronous fluorescence data and ultraviolet data.

3. Results and discussion

3.1. Recirculation ratio

The effect of different recirculation ratios on nitrogen removal performance is shown in Table 1. The COD, NH_3 -N, and TN removal efficiencies were 88.9, 92.8, and 48.4%, respectively when the recirculation ratio between hydrolytic reactor and aerobic reactor was 1/3, which were much higher than those with 1/2 and 1/4 recirculation ratio. The results suggested that a recirculation ratio of 1/3 was optimal to achieve the highest removal efficiencies of COD and nitrogen. The sewage recirculation would promote nitrogen removal by providing carbon sources and nitrate from accumulation for denitrification, which was similar to previous studies [1,10,27]. According to Deng et al. (2007), the removal efficiencies of COD and NH_4^+ -N were only 60–50% using SBR to treat digested effluent adding raw swine wastewater or alkali, which was as effective as those in this study [1].

3.2. Organic acids

As shown in Fig. 2, only formic acid, acetic acid and propanoic acid were detected in the hydrolytic acidification period. The highest concentration of total organic acids appeared at 2 h in the hydrolytic acidification reactor after influent and at the beginning of recirculation, respectively. The concentrations of total organic acids began to decrease firstly along with hydrolytic time and then keep stable after 5 h. The results indicated that macromolecular organic matters were degraded into low molecular organic acids rapidly at the beginning of hydrolytic phase [28], which was suggested by the fast increase in the concentration of total organic acids in the first 2 h after

Table 1
Effect of different circle rates on treatment efficiency

Recirculation ratio	Sample	COD (mg L ⁻¹)	NH ₃ -N (mg L ⁻¹)	TN (mg L ⁻¹)
1:2	Influent	1,884.7	415.4	441.7
	Effluent	208.6	29.9	228.1
	Removal efficiency (%)	88.9%	92.8%	48.4%
1:3	Influent	1,676.5	333.0	473.5
	Effluent	198.1	3.6	105.5
	Removal efficiency (%)	88.2%	98.9%	77.7%
1:4	Influent	1,811.2	398.5	412.8
	Effluent	241.0	54.9	253.5
	Removal efficiency (%)	86.7%	86.2%	38.6%

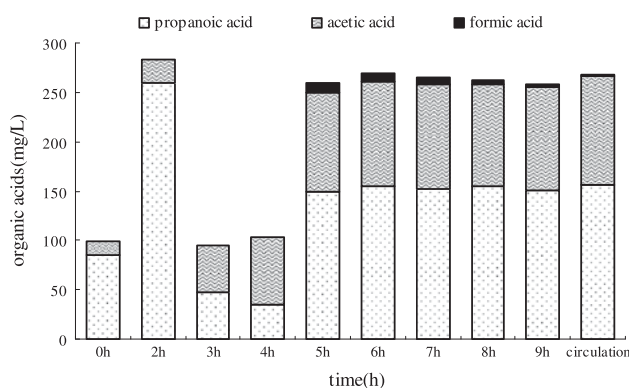


Fig. 2. Variation of organic acids in hydrolytic acidification period before recirculation.

influent. Moreover, it could be observed that propanoic acid concentration began to decrease as acetic acid concentration increased during the first 4 h after influent. This result suggested that propanoic acid was further degraded due to the increasing activity of acid-producing bacteria. Acetic acid and propanoic acid contributed to the main fraction of organic acids produced in hydrolytic phase.

As shown in Fig. 3, formic acid concentration increased after recirculation and then quickly decreased. Acetic acid and propanoic acid concentrations decreased initially and then maintained stable concentration during the final 6 h after recirculation. The results indicated that it would be possible to produce stable acetic acid and propanoic acid concentrations after recirculation. It has been reported that formic acid produced in the hydrolytic acidification reactor could be considered as carbon source to increase nitrogen removal [29,30]. It is also well

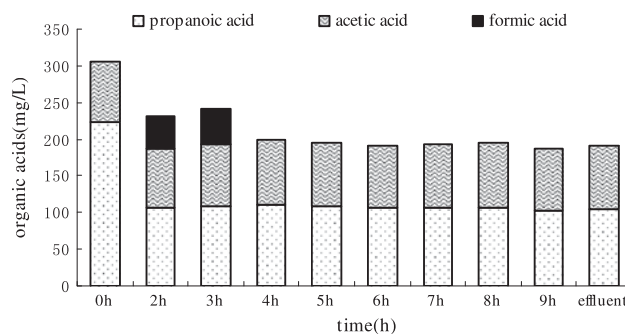


Fig. 3. Variation of organic acids in hydrolytic acidification period after recirculation.

known that acetic acid and propanoic acid could promote both phosphorus absorption and COD removal [31–33]. In this study, recirculation between the two reactors with highest total organic acids concentration could improve the removal efficiency of COD and nitrogen. The results suggested that cyclic organics, saturated and unsaturated fatty acids could be degraded by anaerobic microorganisms and acidogenic bacteria [34]. Consequently, the process of hydrolytic acidification was a suitable pretreatment for digested piggery wastewater, increasing biodegradability, and providing enough carbon sources.

3.3. Fluorescence spectra

3.3.1. Synchronous fluorescence spectra

Synchronous fluorescence spectra of the wastewater samples collected from the two reactors have been measured in order to evaluate structure and components of DOMs [35,36]. A typical synchronous fluorescence spectrum of wastewater samples in

hydrolytic acidification reactor was shown in Fig. 4. In this study, a high-intensity fluorescence peak was clearly identified ranging from 250 to 280 nm, which was associated with protein-like substances. Similar results were shown in previous study, where high-intensity fluorescence peak at 280 nm of sewage effluent was identified due to biodegradable aromatic amino acids [37]. In addition, three low-intensity fluorescence peaks from 330 to 340 nm, 350 to 370 nm, and 460 to 490 nm were identified, which were related to humic substances [38]. The distribution of those peaks indicated that a host of imponderable high molecular weight polycyclic aromatic and humic substances could be degraded into protein-like compounds by anaerobic microorganism and acidogenic bacteria in hydrolytic acidification process. It is quite possible, therefore, that the intensity of protein-like peak could be used for a quantitative estimate of biodegradable constituents with appropriate calibration.

In the biological contact oxidation reactor, protein-like peak and fulvic-like peak also appeared at the same fluorescence areas, as shown in Fig. 5. However, the intensities of the four broad peaks were much lower than those in the hydrolytic acidification reactor. Moreover, a relatively obvious humic-like peak was found due to the accumulation of refractory organic matters in aerobic phase. The reducing intensities of protein-like substances in biological contact oxidation reactor contrasting with those in hydrolytic acidification reactor were nearly within 70%, which has been considered to be an indicator of the high degradation efficiency of aerobic microorganism in biological contact oxidation reactor.

The variation of protein-like peak at 277 nm in the hydrolytic acidification and biological contact oxidation reactor before and after recirculation during synchronous fluorescence is shown in Fig. 6(a)–(d). The intensity of protein-like peak increased with the

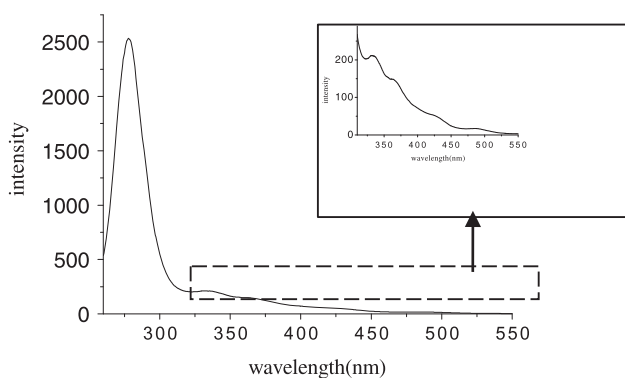


Fig. 4. Synchronous fluorescence spectra of DOM in hydrolytic acidification effluent.

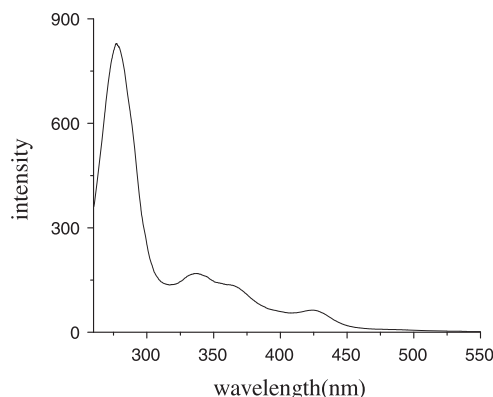


Fig. 5. Synchronous fluorescence spectra of DOM in aerobic effluent.

reaction time and reached the highest point at 2 h after influent, which was consistent with the variation of total organic acids concentration at 2 h before recirculation. The correlation of fluorescence intensity at 277 nm and the total organic acids concentration before and after recirculation were significant with $R^2 = 0.6842$ ($p = 0.003$) and $R^2 = 0.5694$ ($p = 0.012$). The results suggest that small molecular organic acids produced in hydrolytic acidification reactor were the main protein-like substances, which are easily degraded in aerobic phase. Therefore, it was recommended that synchronous fluorescence spectra could be used to analyze qualitatively total the concentration variation of organic acids in hydrolytic acidification reactor. In Fig. 6(c) and (d), intensity of protein-like peak decreased with the reaction time, indicating that simple organic matters were highly degraded in aerobic phase.

The application of synchronous fluorescence spectra analysis has confirmed that the decline of total organic acids concentration should be attributed to formation and degradation of protein-like substances. It is further demonstrated that there were still some refractory organic substances that could not be degraded during the hydrolytic acidification and biological contact oxidation process.

3.3.2. Three-dimensional EEM fluorescence

The three-dimensional EEM fluorescence spectra of DOM samples in hydrolytic acidification reactor before and after recirculation are illustrated in Figs. 7 and 8. Two main peaks could be identified in hydrolytic acidification reactor before recirculation. The first main peak was located at the excitation/emission wavelengths (E_x/E_m) of 240–270 nm/300–350 nm (Peak A), while the second main peak was observed at the

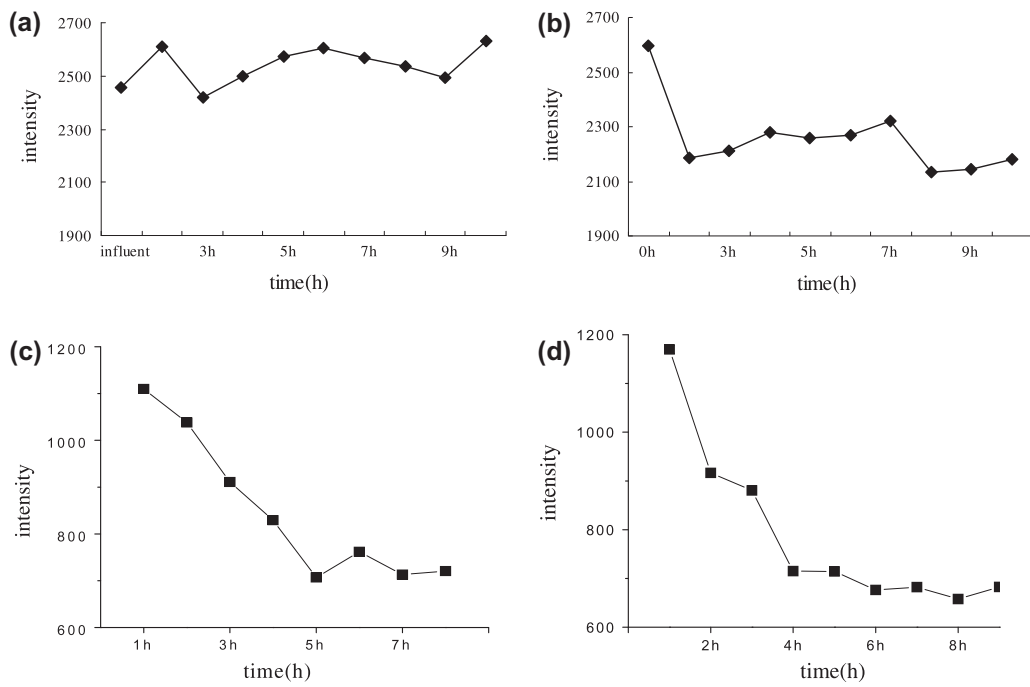


Fig. 6. The variation of synchronous fluorescence intensity of DOM at 277 nm in the two reactions (a) hydrolytic acidification before recirculation; (b) hydrolytic acidification after recirculation; (c) aerobic reactor before recirculation; (d) aerobic reactor after recirculation.

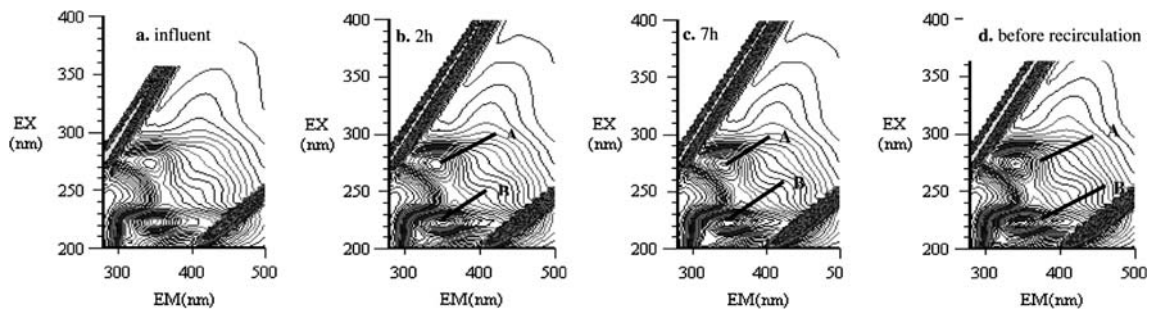


Fig. 7. Fluorescence spectra of DOM in hydrolysis stage before recirculation.

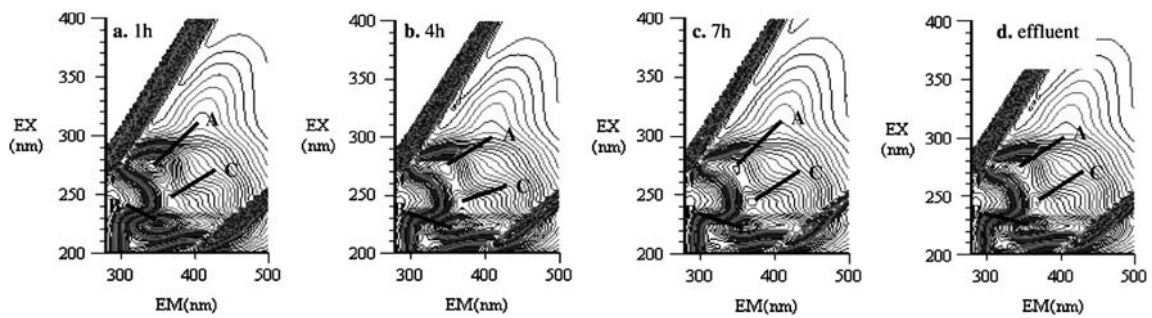


Fig. 8. Fluorescence spectra of DOM in hydrolysis stage after recirculation.

E_x/E_m of 220–240 nm/280–300 nm (Peak B). In general, peaks at shorter excitation wavelengths (<250 nm) and shorter emission wavelengths (<350 nm) are related to simple aromatic proteins [39,40]. The two peaks have been reported as protein-like peaks degraded by microorganisms [35,41]. The protein-like fluorescence intensity increased with the reaction time, indicating complex DOM was degraded into simple compounds. After recirculation, another protein-like peak at the E_x/E_m of 250–260 nm/320–350 nm (Peak C) was identified as shown in Fig. 8, which were associated with soluble microbial byproduct-like material coming from aerobic reactor [42,43]. The intensity of Peak C increased along with the reaction time, while the intensities of Peak A and Peak B decreased. The fluorescence intensity (FI) of the peaks provided some useful information on the variation of DOM during hydrolytic acidification process. The general FI decreasing in Peak A and Peak B with hydrolytic time may be related to the extensive decomposition of DOM. The slowly increasing FI of peak C may be due to the increased probability of electron transition between singlet and ground state. This effect would result in an increased refractory compounds associated with aromatic structures and conjugated double bonds of higher thermodynamic stability. These results suggest that the recirculation between two

reactors accelerated the decomposition of simple organic matters and production of complicated organic matters simultaneously. Furthermore, sewage recirculation from biological contact oxidation reactor brought abundant low molecular organic acids into the hydrolytic phase, providing enough carbon sources and nitrate for denitrification.

Figs. 9 and 10 presented the variation of three-dimensional EEM fluorescence spectra of DOM in biological contact oxidation reactor before and after recirculation. It could be observed that three main peaks at the E_x/E_m of 210–230 nm/340–360 nm (Peak A), E_x/E_m of 270–280 nm/340–380 nm (Peak B), E_x/E_m of 310–340 nm/420–440 nm (Peak D) were identified in the whole aerobic process. Obviously, both Peak A and Peak B represented protein-like substances, and Peak D was related to fulvic acid-like organic matters [44], which had a red-shifted from protein-like peak to fulvic acid-like peak due to the production of refractory organic matters in the aerobic process. According to the previous study, a red shift is associated with the compounds containing carboxyl constituents, hydroxyl, alkoxy, amino groups, and carboxyl constituents [45]. It could be concluded that fulvic acid-like substances mainly accounts for accumulation of refractory organic matters in the aerobic process. Also, some non-degraded large molecular organic com-

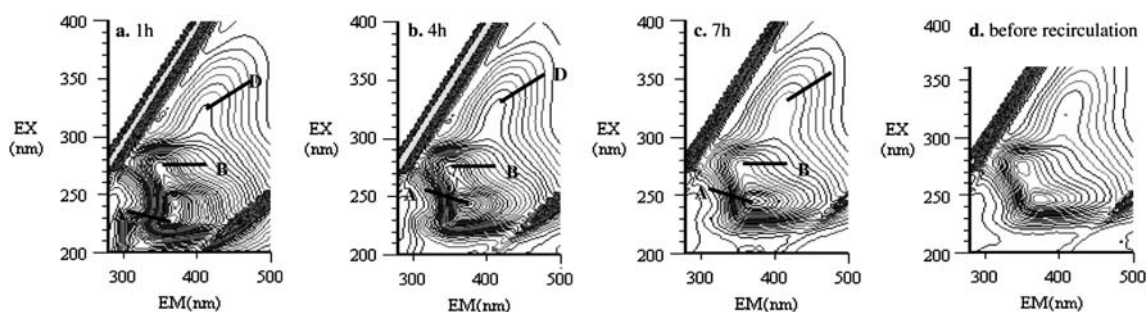


Fig. 9. Fluorescence spectra of DOM in aerobic stage before recirculation.

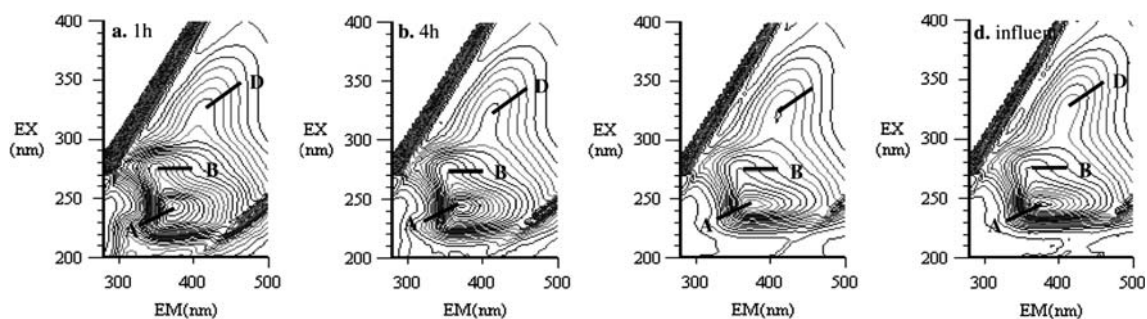


Fig. 10. Fluorescence spectra of DOM in aerobic stage after circulation.

pounds could be decomposed in hydrolytic acidification after recirculation from biological contact oxidation reactor to hydrolytic acidification reactor. During aeration, the intensity of protein-like peak decreased because of microorganism degradation and the intensity of fulvic acid-like peak increased gradually, which indicates fulvic substances accumulated in the last phase of aerobic reaction. Therefore, protein-like substances were easily degraded into low molecular compounds in aerobic phase by aerobic microorganisms rather than fulvic acid-like substances.

3.4. Ultraviolet spectrum

3.4.1. Variation of UV absorption spectra

In order to better understand characteristics variations of DOM in hydrolytic acidification and biological contact reactors, the UV absorption analysis were also conducted (Figs. 11 and 12). It can be seen that the UV absorbance in the hydrolytic acidification and biological contact oxidation reactor before recirculation decreased along with the increment of wave-

length. All sewage samples in different reaction time have strong absorption at 280 nm, where lignin sulphonates and their derivatives absorbed [46]. Furthermore, UV absorption at 280 nm could also be attributed to DOC and aromatic organic compounds [47]. The variation of aromaticity and unsaturation of fulvic-like materials in hydrolytic acidification increased with the reaction time while the tendency was opposite in the biological contact oxidation reactor. The results indicate that degradation of aromatic compounds in hydrolytic acidification reactor is more obvious than those in the biological contact oxidation reactor. Moreover, there was nitrate absorption between 200 and 260 nm during the reaction, especially in the aerobic reactor. It could be speculated that sewage recycled from biological contact oxidation reactor accounts for the presence of nitrate in the hydrolytic acidification reactor, while high nitrification efficiency was obtained in the biological contact oxidation reactor. The results suggested that denitrification efficiency in the hydrolytic acidification reactor

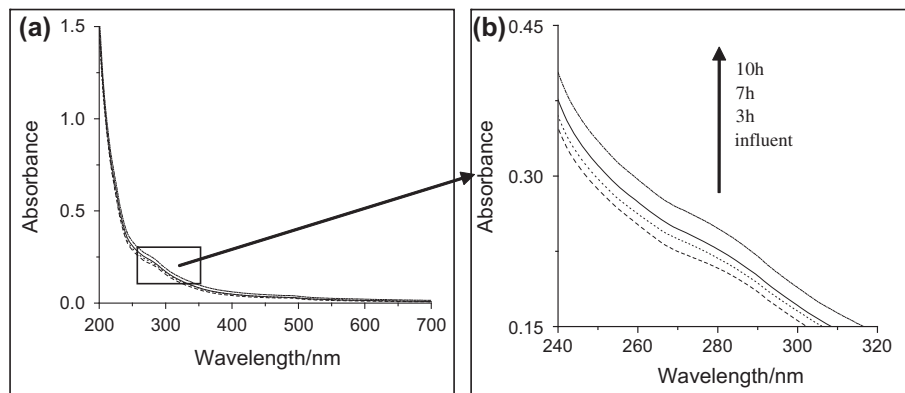


Fig. 11. UV-spectra of DOM in hydrolysis stage.

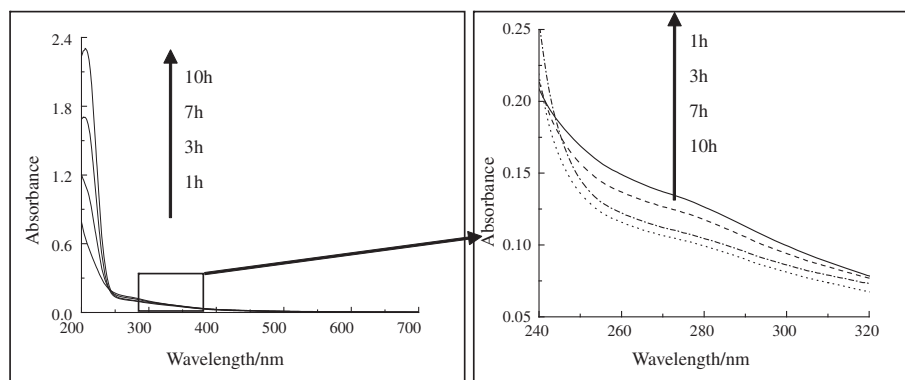


Fig. 12. UV-spectra of DOM in aerobic stage.

was low before recirculation because of nitrate accumulation.

3.4.2. Variation of $SUVA_{254}$ and E_{253}/E_{203}

The variations of $SUVA_{254}$ and E_{253}/E_{203} with the reaction time during hydrolytic acidification and biological contact oxidation processes were shown in Figs. 13 and 14. In Fig. 13, the increasing tendency of $SUVA_{254}$ and E_{253}/E_{203} indicated that much more kinds of aromatic compounds and substituents on aromatic ring were produced during hydrolytic acidification process, which could be easily degraded in biological contact oxidation reactor. The increasing types and quantities of substituents on aromatic ring were mainly from decomposition of macromolecular organic matters. It could be concluded that compounds containing aliphatic substituents were the main fractions of DOM at the beginning of hydrolytic phase, and most of them were gradually replaced by either carbonyl, carboxyl, or hydroxyl along with the reaction time. Those compounds were easily degraded in aerobic phase. In Fig. 14, the opposite tendency of

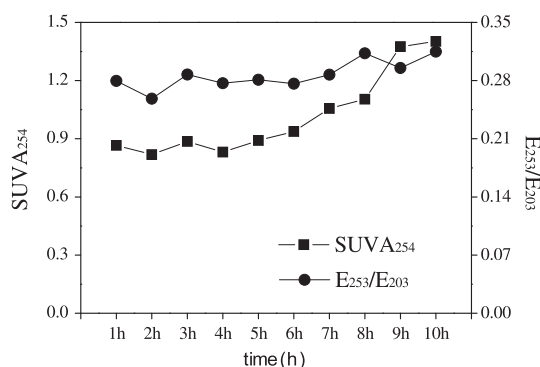


Fig. 13. $SUVA_{254}$, E_{253}/E_{203} of DOM in hydrolysis stage.

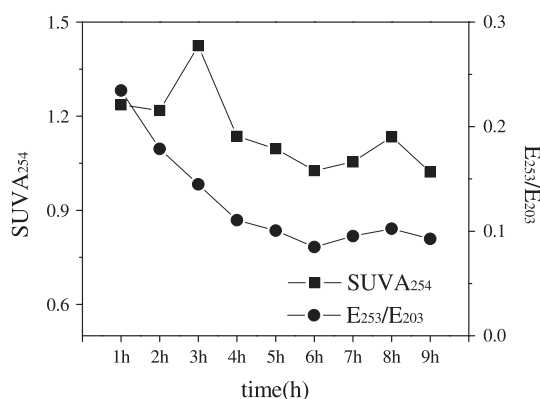


Fig. 14. $SUVA_{254}$, E_{253}/E_{203} of DOM in aerobic stage.

$SUVA_{254}$ and E_{253}/E_{203} could be found due to the degradation of low molecular substances along with the aerobic reaction time. It was also found that variation of $SUVA_{254}$ and E_{253}/E_{203} tended to be stable after 6 h in aerobic phase indicating the maximum utilization rate of total organic acids was present at this time, which was similar with the results in Fig. 6 (d). Based on these results, it could be suggested that DOM molecular structure varied from complex long-chain aromatic ring substituents (e.g. aliphatic chain) to simple short-chain aromatic ring substituents (e.g. carbonyl, carboxyl, hydroxyl, and ester).

4. Conclusion

DOM samples of digested piggery wastewater treatment in hydrolytic acidification and biological contact oxidation reactors were characterized by ion chromatography, fluorescence spectroscopy and UV spectra. The highest removal efficiency of COD and nitrogen could be achieved at 1/3 recirculation ratio, and the removal efficiencies were 88.2% and 98.9% for COD and NH_3-N , respectively. The highest total organic acids concentration in hydrolytic acidification reactor was achieved at 2 h after influent and after the beginning of recirculation, respectively. The results of synchronous fluorescence indicated that intensity of protein-like peak at 277 nm was significantly correlated with the total organic acids concentration. It was also found that protein-like substances were the main fractions of DOM in hydrolytic phase, and the accumulation of refractory organic matters was present in aerobic phase. The EEM fluorescence spectra indicated three protein-like peaks of DOM samples from hydrolytic acidification phase were identified before and after recirculation, respectively. Moreover, fulvic-like peak was identified and its intensity increased with the reaction time in aerobic reactor. The results of $SUVA_{254}$ and E_{253}/E_{203} variations indicated that aromaticity and unsaturation of DOM in sewage increased with hydrolytic time, and the types and quantities of substituents on aromatic ring also increased, which was suitable to subsequent aerobic treatment.

Acknowledgements

This study is supported by the National Natural Science Foundation of China (No. 40901248), the Mega-projects of Science Research for Water Environment Improvement (Program Nos. 2009ZX07106-001, 2012ZX07101-002) and the China Basic Research Program (Program No. 2008CB418206). We are grateful for the three anonymous reviewers for their constructive comments and suggestions on the manuscript.

References

- [1] L.W. Deng, P. Zhang, Z. Chen, Q. Mahmood, Improvement in post-treatment of digested swine wastewater, *Bioresour. Technol.* 99(8) (2007) 3136–3145.
- [2] X.M. Wei, C. Lin, N. Duan, Y.X. Penga, Z.Y. Ye, Application of aerobic biological filter for treating swine farms wastewater, *Proc. Environ. Sci.* 2 (2010) 1569–1584.
- [3] T. Osada, K. Haga, Y. Harada, Removal of nitrogen and phosphorus from swine wastewater by activated sludge units with the intermittent aeration process, *Water Res.* 25(11) (1991) 1377–1388.
- [4] J.R. Bicudo, I.F. Svobada, Intermittent aeration of pig slurry farm scale experiments for carbon and nitrogen removal, *Water Sci. Technol.* 32(12) (1995) 83–90.
- [5] G. Bortone, S. Gemelli, A. Rambaldi, Nitrification, denitrification and biological phosphate removal in sequencing batch reactors treating piggery wastewater, *Water Sci. Technol.* 26 (5–6) (1992) 977–985.
- [6] L. Fernandes, E. Mckyes, M. Warith, S. Barrington, Treatment of liquid swine manure in the sequencing batch reactor under aerobic and anoxic condition, *Canadian Agric. Eng.* 33(2) (1991) 373–379.
- [7] K.V. Lo, P.H. Liao, R.J. Van Kleek, A full-scale sequencing batch reactor treatment of dilute swine wastewater, *Canadian Agric. Eng.* 33(1) (1991) 193–195.
- [8] J.J. Su, C.M. Kung, J. Lin, W.C. Lian, J.F. Wu, Utilization of sequencing batch reactor for *in situ* piggery wastewater treatment, *J. Environ. Sci. Health* 32(2) (1997) 391–405.
- [9] B.D. Edgerton, D. McNevin, C.H. Wong, P. Menoud, J.P. Barford, C.A. Mitchell, Strategies for dealing with piggery effluent in Australia: The sequencing batch reactor as a solution, *Water Sci. Technol.* 41(1) (1999) 123–126.
- [10] J.Y. Cheng, B. Liu, Nitrification/denitrification in intermittent aeration process for swine wastewater treatment, *J. Environ. Eng.* 127(8) (2001) 705–711.
- [11] D. Obaja, S. Macé, J. Costa, C. Sans, J. Mata-Alvarez, Nitrification, denitrification and biological phosphorus removal in piggery wastewater using sequencing batch reactor, *Bioresour. Technol.* 87(1) (2003) 103–111.
- [12] Z.J. Zhang, J. Zhu, J. King, W.H. Li, A two-step fed SBR for treating swine manure, *Process Biochem.* 41(4) (2006) 892–900.
- [13] J. Kim, M. Chen, N. Kishida, R. Sudo, Integrated real-time control strategy for nitrogen removal in swine wastewater treatment using sequencing batch reactors, *Water Res.* 38(14–15) (2004) 3340–3348.
- [14] C.S. Ra, K.V. Lo, D.S. Mavinic, Real-time control of two-stage sequencing batch reactor system for the treatment of animal wastewater, *Environ. Technol.* 19(4) (1998) 343–356.
- [15] A. Tilche, E. Bacilieri, G. Bortone, F. Malaspina, S. Piccinini, L. Stante, Biological phosphorus and nitrogen removal in a full scale sequencing batch reactor treating piggery wastewater, *Water Sci. Technol.* 40(1) (1999) 199–206.
- [16] C.M. Liao, T. Maekawa, Nitrification/denitrification in an intermittent aeration process for swine by the rotating disc system, *J. Environ. Sci. Health (Part B)*, 29(5) (1994) 1053–1078.
- [17] J. Chen, E.J. LeBoeuf, S. Dai, B.H. Gu, Fluorescence spectroscopic studies of natural organic matter fractions, *Chemosphere* 50(5) (2003) 639–647.
- [18] A. Cilenti, M.R. Provenzano, N. Senesi, Characterization of dissolved organic matter from saline soils by fluorescence spectroscopy, *Environ. Chem. Lett.* 3(2) (2005) 53–56.
- [19] S.L. Huo, B.D. Xi, H.C. Yu, L.S. He, S.L. Fan, Characteristics of dissolved organic matters (DOM) in leachate with different landfill ages, *J. Environ. Sci.* 20(4) (2008) 492–498.
- [20] A. Baker, M. Curry, Fluorescence of leachates from three contrasting landfills, *Water Res.* 38(10) (2004) 2605–2613.
- [21] A. Baker, Thermal fluorescence quenching properties of dissolved organic matter, *Water Res.* 39(18) (2005) 4405–4412.
- [22] K. Hayakawa, T. Sekino, T. Yoshioka, M. Maruo, M. Kumagai, Dissolved organic carbon and fluorescence in Lake Hovsgol: Factors reducing humic content of the lake water, *Limnology* 4(1) (2003) 26–33.
- [23] J.J. Macauley, Z.M. Qiang, C.D. Adams, R. Surampalli, M.R. Mormile, Disinfection of swine wastewater using chlorine, ultraviolet light and ozone, *Water Res.* 40(10) (2006) 2017–2026.
- [24] X.Q. Lu, R. Jaffe, Interaction between Hg(II) and natural dissolved organic matter: A fluorescence spectroscopy based study, *Water Res.* 35(7) (2001) 1793–1803.
- [25] W. Nishijima, G.E. Speitel, Fate of biodegradable dissolved organic carbon produced by ozonation on biological activated carbon, *Chemosphere* 56(2) (2004) 113–119.
- [26] J.Z. Zhang, Q. Yang, B.D. Xi, Z.M. Wei, X.S. He, M.X. Li, T.X. Yang, Study on spectral characteristic of dissolved organic matter fractions extracted from municipal solid waste landfill leachate, *Spectrosc. Spectral Anal.* 28(11) (2008) 2583–2587 (in Chinese).
- [27] D.S. Obaja, J. Mace, J. Mata-Alvarez, Biological nutrient removal by a sequencing batch reactor (SBR) using an internal organic carbon source in digested piggery wastewater, *Bioresour. Technol.* 96(1) (2005) 7–14.
- [28] S.U. Ahmed, H. Mogens, Biological hydrolysis and acidification of sludge type and origin on the production and composition of volatile fatty acids, *Water Res.* 42(14) (2008) 3729–3738.
- [29] L. Qin, Y. Liu, Aerobic granulation for organic carbon and nitrogen removal in alternating aerobic–anaerobic sequencing batch reactor, *Chemosphere* 63(6) (2006) 926–933.
- [30] S.F. Yang, J.H. Tay, Y. Liu, A novel granular sludge sequencing batch reactor for removal of organic and nitrogen from wastewater, *J. Biotechnol.* 106(1) (2003) 77–86.
- [31] Y.G. Chen, Y.S. Chen, Q. Xu, Q. Zhou, G.W. Gu, Comparison between acclimated and unacclimated biomass affecting anaerobic–aerobic transformations in the biological removal of phosphorus, *Process Biochem.* 40(2) (2005) 723–732.
- [32] Y.G. Chen, A.A. Randall, T. McCue, The efficiency of enhanced biological phosphorus removal from real wastewater affected by different ratio of acetic to propionic acid, *Water Res.* 38(1) (2004) 27–36.
- [33] F. Omil, P. Lens, L.H. Pol, G. Lettinga, Effect of upward velocity and sulphide concentration on volatile fatty acid degradation in a sulphidogenic granular sludge reactor, *Process Biochem.* 31(7) (1996) 699–710.
- [34] M. Beccari, M. Majone, L. Torrisi, Two-reactor system with partial phase separation for anaerobic treatment of olive oil mill effluents, *Water Sci. Technol.* 38(4–5) (1998) 53–60.
- [35] W. Chen, P. Westerhoff, J.A. Leenheer, K. Booksh, Fluorescence excitation–emission matrix regional integration to quantify spectra for dissolved organic matter, *Environ. Sci. Technol.* 37(24) (2003) 5701–5710.
- [36] J. Hur, G. Kim, Comparison of the heterogeneity within bulk sediment humic substances from a stream and reservoir via selected operational descriptors, *Chemosphere* 75(4) (2009) 483–490.
- [37] S.R. Ahmad, D.M. Reynolds, Synchronous fluorescence spectroscopy of wastewater and some potential constituents, *Water Res.* 29(6) (1995) 1599–1602.
- [38] X.D. Ma, S.A. Green, Fractionation and spectroscopic properties of fulvic acid and its extract, *Chemosphere* 72(10) (2008) 1425–1434.
- [39] S.R. Ahmad, D.M. Reynolds, Monitoring of water quality using fluorescence technique: Prospect of on-line process control, *Water Res.* 33(9) (1999) 2069–2074.
- [40] S. Determann, R. Reuter, P. Wagner, R. Willkomm, Fluorescent matter in the eastern Atlantic Ocean, Part 1: Method of measurement and near-surface distribution, *Deep Sea Res. Part 1: Oceanogr. Res. Papers* 41(4) (1994) 659–675.

- [41] J.A. Leenheer, J.P. Croue, Characterizing aquatic dissolved organic matter, *Environ. Sci. Technol.* 37(1) (2003) 19–26.
- [42] P.G. Coble, Characterization of marine and terrestrial DOM in seawater using excitation–emission matrix spectroscopy, *Marine Chem.* 51(4) (1996) 325–346.
- [43] D.M. Reynolds, S.R. Ahmad, Rapid and direct determination of wastewater BOD values using a fluorescence technique, *Water Res.* 31(8) (1997) 2012–2018.
- [44] J. David, S.W.K. Burdige, W.H. Chen, Fluorescent dissolved organic matter in marine sediment pore waters, *Marine Chem.* 89(1–4) (2004) 289–311.
- [45] J. Chen, B. Gu, E.J. Leboeuf, H. Pan, S. Dai, Spectroscopic characterization of the structural and functional properties of natural organic matter fractions, *Chemosphere* 48(1) (2002) 59–68.
- [46] J. Zhang, J. Cao, S. Tao, Spatial variation of UV–VIS spectroscopy of water soluble organic carbon in eastern china, *Acta Pedol. Sinica* 40(1) (2003) 118–122 (in Chinese).
- [47] S. Magnus, K. Klaus, D. Rolf, F. Andreux, J. Ranger, Estimating nitrate, dissolved organic carbon and DOC fractions in forest floor leachates using ultraviolet absorbance spectra and multivariate analysis, *Geoderma* 124(1–2) (2005) 157–168.